The effect of hyperthermia on the DNA damage response induced by γ-rays, as determined through *in situ* cell tracking

Qibin Fu[1], Jing Wang[2] and Tuchen Huang[1],*

[1]Sino-French Institute of Nuclear Engineering and Technology, Sun Yat-sen University, Tang Jia Wan, Zhuhai 519082, P. R. China
[2]State Key Laboratory of Nuclear Physics and Technology, School of Physics, Peking University, Beijing 100871, P. R. China
*Corresponding author. Sino-French Institute of Nuclear Engineering and Technology, Sun Yat-sen University, Tang Jia Wan, Zhuhai 519082, P.R.China.
Tel: +8607563668967; Email: huangtuchen@mail.sysu.edu.cn
(Received 6 May 2018; revised 29 May 2018; editorial decision 29 June 2018)

ABSTRACT

Hyperthermia (HT) acts as a cancer treatment by direct cell killing, radiosensitization, and promotion of tumor reoxygenation. The sensor proteins of the DNA damage response (DDR) are the direct targets of HT. However, the spatiotemporal properties of sensor proteins under HT are still unclear. Therefore, investigating the impact of HT on sensor proteins is of great importance. In the present study, the human fibrosarcoma cell line HT1080 stably transfected with 53BP1-GFP [the DDR protein 53BP1 fused to green fluorescent protein (GFP)] was used to investigate the real-time cellular response to DNA double-strand breaks (DSBs) induced by γ-rays. Using live-cell imaging combined with HT treatment, the spatiotemporal properties of the 53BP1 protein were directly monitored and quantitatively studied. We found that HT could delay and decrease the formation of 53BP1 ionizing radiation–induced foci (IRIF). Moreover, through the *in situ* tracking of individual IRIF, it was found that HT resulted in more unrepaired IRIF over the period of observation compared with IR alone. Additionally, the unrepaired IRIF had a larger area, higher intensity, and slower repair rate. Indeed, almost every cell treated with HT had unrepaired IRIF, and the majority of these IRIF increased in area individually, while the rest increased in area by the merging of adjacent IRIF. In summary, our study demonstrated that HT could perturb the primary event in the DDR induced by IR, and this may have important implications for cancer treatment and heat radiosensitization.

Keywords: γ-irradiation; hyperthermia; live-cell imaging; DNA damage response; single IRIF analysis

INTRODUCTION

Hyperthermia (HT) therapy, through increasing the temperature of tumor-loaded tissue to 40–43°C, is often applied as an adjuvant to radiotherapy [1, 2]. HT acts as a cancer treatment by direct cell killing, radiosensitization, and promotion of tumor reoxygenation [2]. The impact of HT on the DNA damage response (DDR) and repair is important for cancer treatment.

Accumulating evidence has shown that various DNA repair systems are targets of HT. For instance, HT could inactivate DNA-polymerase β, which is the key enzyme in base excision repair [3]. For the repair of ionizing radiation (IR)-induced DNA double-strand breaks (DSBs), there are two main pathways, namely, non-homologous end joining (NHEJ) and homologous recombination (HR) [4]. HT has a great impact on NHEJ through the aggregation of Ku protein, which leads to the inactivation of the DNA-binding activity [5]. The effects of HT on HR are even more pronounced and diverse. Heat stress (42–45°C) could induce the translocation of MRN complex (Mre11/Rad50/Nbs1) from the nucleus to the cytoplasm [6]. Moreover, the recruitment of recombinase Rad51 and protein BRCA2 are blocked at 40–42°C [7, 8].

In addition, several sensor proteins are the direct targets of HT. Based on immunofluorescent analysis, HT before or after IR could delay the formation of 53BP1 complex [9]. However, traditional measurements can not reveal the dynamics of DDR within a single cell. Thus, the spatiotemporal properties of sensor proteins under HT are being discussed.

In the present study, we used human fibrosarcoma cell line HT1080 stably transfected with 53BP1-GFP [the DDR protein 53BP1 fused to green fluorescent protein (GFP)] as a DSB surrogate marker. Additionally, the confocal microscope used was equipped with a temperature chamber and CO_2 module for HT treatment. Thus, the spatiotemporal properties of sensor proteins treated with HT could be directly monitored and quantitatively studied. Using time-lapse imaging, we found that HT could delay and decrease the formation of 53BP1 IR-induced foci (IRIF). Moreover, through the *in situ* tracking of individual IRIF, it was observed that HT resulted in more unrepaired IRIF over the period of observation compared with treatment with IR alone. Additionally, the unrepaired IRIF had a larger area and a higher intensity as well as a slower repair rate. It is noteworthy that almost every cell treated with HT had unrepaired IRIF, and the majority of these IRIF increased in area individually, while the rest increased in area by the merging of adjacent IRIF. Taken together, the results demonstrated that HT could perturb the primary event in the DDR induced by IR, and this may have important implications for cancer treatment and heat radiosensitization.

MATERIALS AND METHODS
Cell culture
The human fibrosarcoma HT1080 cell line stably transfected with 53BP1-GFP was kindly provided by Dr David J. Chen (University of Texas Southwestern) and has previously been described [10]. The cells were cultured in DMEM high-glucose medium with 10% fetal bovine serum, 100 U/ml penicillin and 100 mg/ml streptomycin, and were incubated at 37°C in an atmosphere of 95% air and 5% CO_2.

Cell treatments
For IR treatment, cells were irradiated by γ-rays from a 2.6 × 10^5 Curie ^{60}Co source at Peking University, with total dose of 1 Gy (dose rate 0.94 Gy/min). For IR+HT treatments, the same IR treatment procedure was performed followed by incubation in a 41°C chamber that was equipped with a confocal microscope (Carl Zeiss LSM700) as previously described [11]. The

temperature was set to 41°C, which had minimal effect on cell viability.

Time-lapse image acquisition
Live cell images were captured immediately after irradiation, using an LSM700 confocal microscope with an EC Plan-Neofluar 40/1.30 oil DIC objective. The laser and filter we used had 488 nm excitation/509 nm emission for GFP. The laser power was typically set to 1–2% transmission with the pinhole opened to 1–2 Airy units. Images were collected at z-stacks (12–14 sections) of 600 nm intervals. The time interval between two successive image acquisitions ranged from several minutes to hours. During imaging, cells were grown in 35-mm glass-bottomed culture dishes maintained in a humidified environmental chamber at 37°C or 41°C.

Image and data processing
Image processing was performed using ImageJ software with manual validation. To visualize all foci and nucleus within one single 2D image, a maximum intensity projection (MIP) of z-stacks was performed. Selected individual foci were tracked, and shape parameters (centroid position, area and mean gray value) were collected.

Statistical analysis
The results were presented as mean ± SD. Significance was assessed using Student's *t*-test, and defined as $P < 0.05$ (significant difference) or $P < 0.01$ (extremely significant difference).

RESULTS
HT delayed and decreased the formation of the 53BP1 IRIF induced by γ-irradiation
To investigate how HT affected the cellular response to DSBs induced by γ-rays, we used HT1080 cells stably transfected with 53BP1-GFP. Because HT alone did not induce 53BP1 foci, as demonstrated in a previous report [12], we could study the effect of HT on the formation of the 53BP1 IRIF induced by γ-rays. Irradiated HT1080 cells were treated at 41°C and imaged simultaneously. Generally, within 5–15 min after exposure to IR, 53BP1 localized at discrete foci [13]. However, 20 min after γ-irradiation,
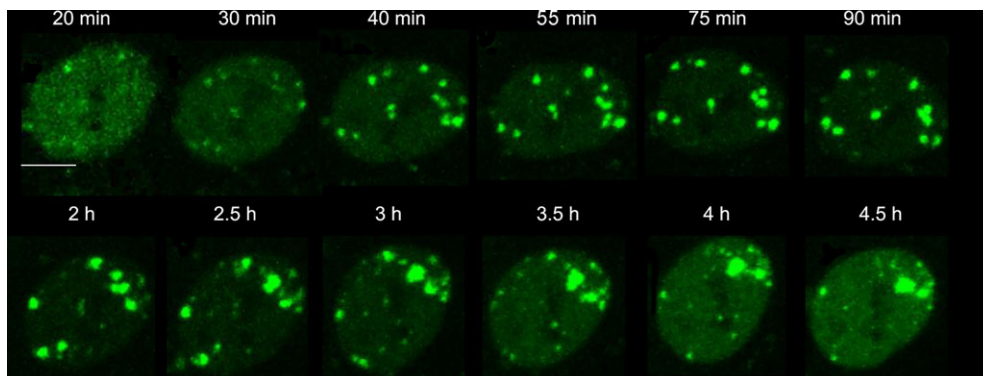

Fig. 1. Representative time-lapse images at 41°C after γ irradiation. Bar = 5 μm.

53BP1 IRIF could only be observed in a few cells under HT treatment. Each selected IRIF was tracked *in situ* from 20 min to several hours after treatments (Fig. 1). In this way, the dynamics of 53BP1 IRIF could be studied.

As shown in Fig. 2A, ~98.6% IRIF in the IR group appeared at 20 min post irradiation, while only 58.6% IRIF existed at that time in the IR+HT group. By 55 min after exposure to the γ-rays, all IRIF had emerged in the IR+HT group (Fig. 2A), indicating the delay in 53BP1 IRIF recruitment. In addition, the number of IRIF per cell treated with or without HT were compared. In the IR group, the number of IRIF reached a peak at 20 min (Fig. 2B). However, the peak time for the IR+HT group was ~40 min (Fig. 2B), also indicating the delay in formation of 53BP1 IRIF. Moreover, the average number of IRIF in the IR+HT group was significantly fewer than that in the IR group $(10 \pm 3/\text{nucleus vs } 24 \pm 6/\text{nucleus}, P < 0.01, \text{Fig. 2B})$. Taken together, the results demonstrated that HT could delay and decrease the formation of 53BP1 IRIF.

Characterization of 53BP1 IRIF in heated–irradiated cells by individual IRIF analysis

In order to further analyze individual IRIF, the maximum values of area and intensity for each IRIF were calculated. As shown in Fig. 3A, no significant difference was detected between the IR group and the IR+HT group with respect to average area $(14 \pm 10$ for the IR group and 13 ± 15 for IR+HT group, $P = 0.75)$ or intensity $(146 \pm 57$ for the IR group and 156 ± 50 for the IR+HT group, $P = 0.06)$. Interestingly, in the IR+HT group, 26% of the IRIF did not disappear at the last observed time point in the present study, which was more than twice that in the IR group. Thus, the IRIF could be divided into two categories, 'disappeared' (i.e. repaired) IRIF and unrepaired IRIF. As shown in Fig. 3B, the recruitment of unrepaired IRIF was clearly delayed compared with that of disappeared IRIF. Additionally, the disappeared IRIF lost half their peak intensity within 80 min, while there was no obvious decrease in the intensity of the

unrepaired IRIF over the period of observation (Fig. 3B). Furthermore, compared with the disappeared IRIF, a significantly larger area $(28 \pm 23$ vs 8 ± 6, $P < 0.01)$ and higher intensity $(200 \pm 15$ vs 141 ± 49, $P < 0.01)$ were observed in the unrepaired IRIF (Fig. 3C). Collectively, the results suggested that larger and brighter IRIF may be associated with the slower repair process.

It is of interest to note that almost every cell treated with HT had unrepaired IRIF. The spatiotemporal properties of each unrepaired IRIF were further analyzed *in situ*. Interestingly, we found that ~83% of these unrepaired IRIF gradually increased in size with time after exposure (Fig. 4A), which was reflective of the persistence of complex DSB lesion, while for the remaining IRIF, the apparent growth in IRIF area was due to the clustering of adjacent IRIF (Fig. 4B). As shown in Fig. 4B, the proximal IRIF clustered in the *x*, *y* and *z* directions.

DISCUSSION

Many studies have shown that HT has a great impact on the response of IR-induced DNA damage. Notably, the sensor proteins of the DDR are the direct targets of HT. Andrei Laszlo *et al.* reported that heat induced the delay of 53BP1 formation, and that this delay was modulated by Hsp 70 protein [9]. However, traditionally, DDR has been investigated using biochemical approaches that are based on measurements of populations of cells. Such measurements cannot reveal the detailed dynamics within a single cell. Also, the effect of HT on the spatiotemporal properties of sensor proteins is difficult to observe. In the present study, we used live-cell imaging to investigate the effect of HT on the spatiotemporal properties of 53BP1 IRIF induced by γ-rays. We found that HT inhibited the response for IR-induced DSBs in HT1080 cells, delaying 53BP1 IRIF formation and reducing the number of IRIF (Fig. 2). Moreover, HT-induced delay in 53BP1 complex formation could perturb the repair of DSBs [14], which would result in a higher probability of the persistence of unrejoined DSBs and/or the generation of misrejoined DSBs [15]. Furthermore, mild hyperthermia
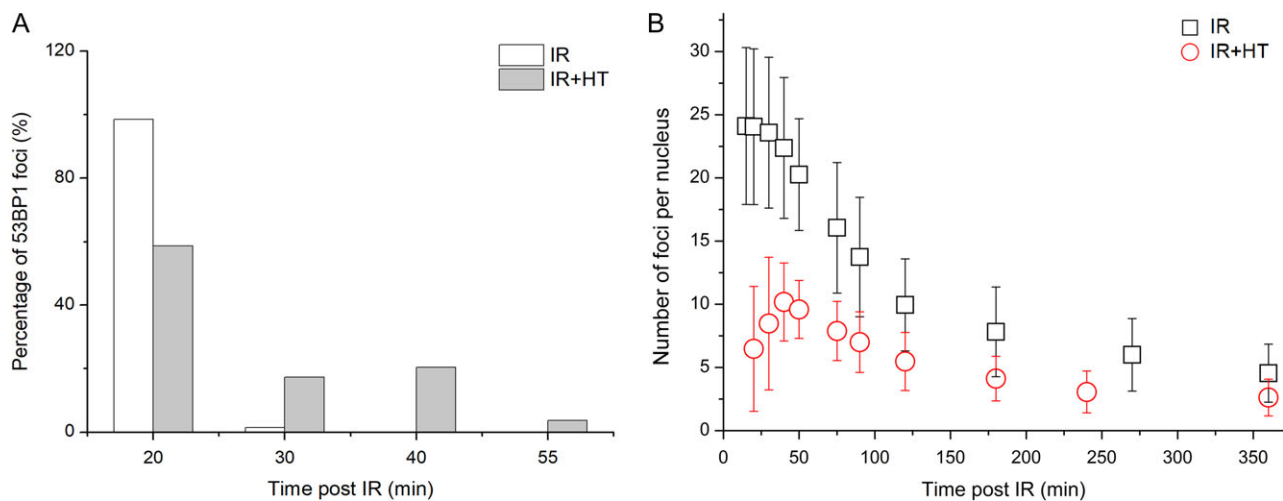

Fig. 2. HT could delay and decrease the formation of 53BP1 IRIF. (A) The percentage of 53BP1 IRIF at indicated times after treatment with IR or IR+HT. (B) The number of IRIF per cell at indicated times after treatment with IR or IR+HT.
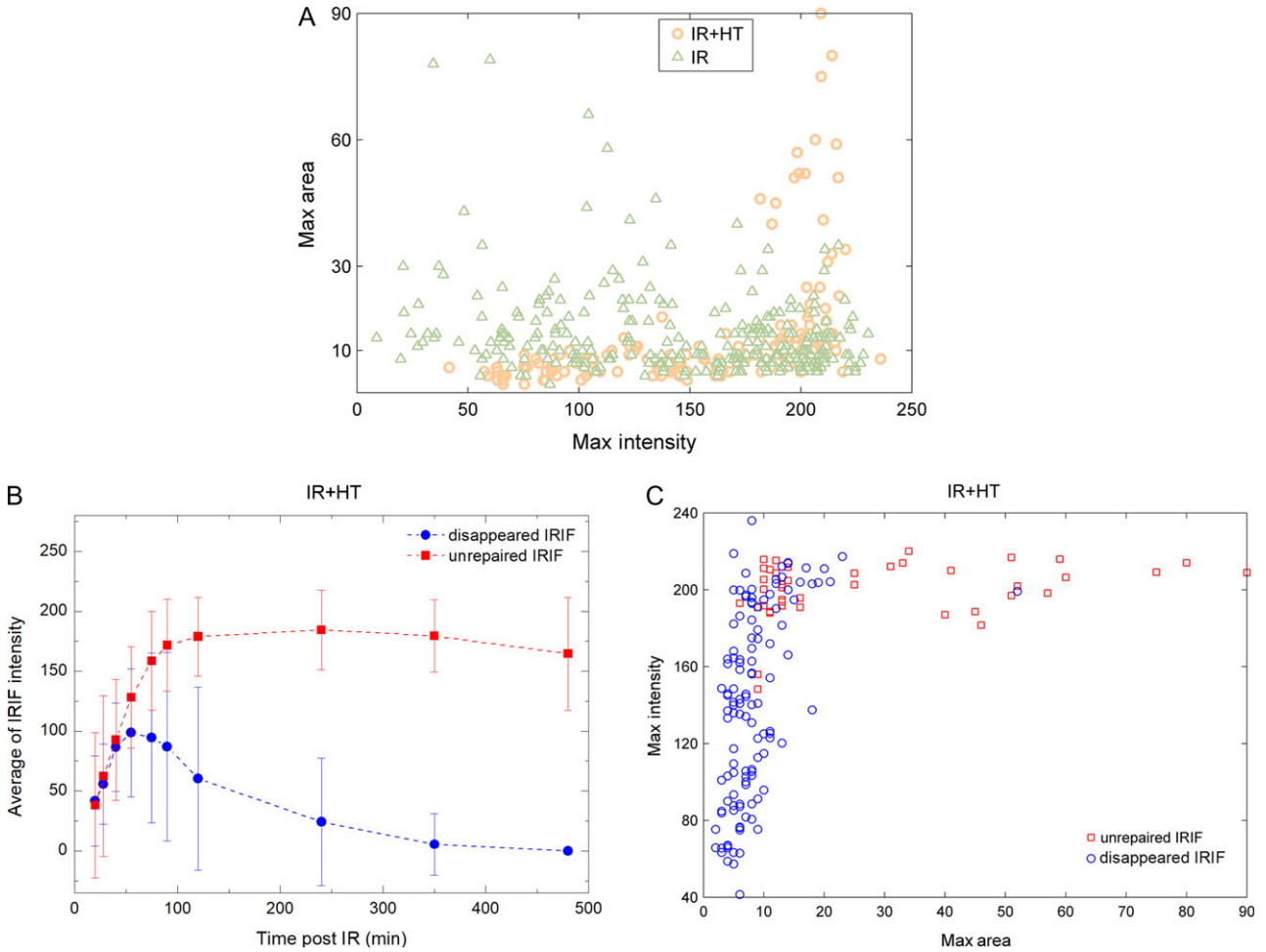
Fig. 3. Analysis of single IRIF. (A) The correlation of maximum IRIF area and maximum IRIF intensity. Orange circles and green triangles represent single IRIF in the IR+HT group and the IR group, respectively. (B) The average intensity of unrepaired IRIF (red squares) and 'disappeared' (i.e. repaired) IRIF (blue dots) in the IR+HT group at indicated times. (C) The correlation of maximum IRIF intensity and maximum IRIF area in the IR+HT group. Red squares and blue circles represent single unrepaired IRIF and 'disappeared' (i.e. repaired) IRIF, respectively.
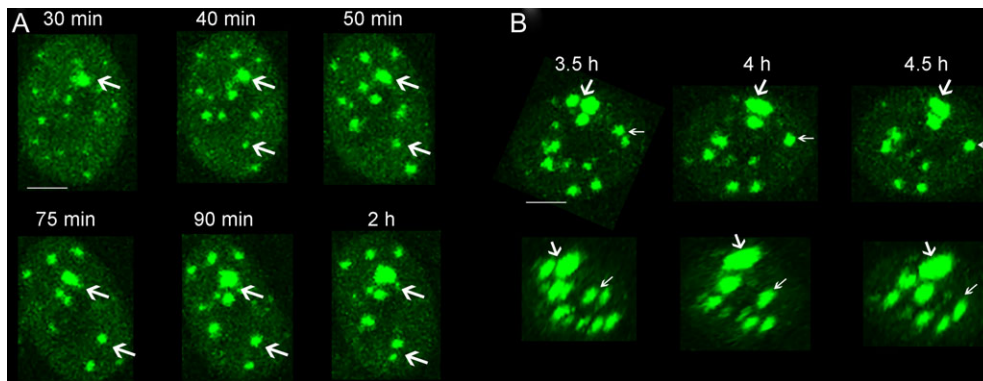

Fig. 4. Different ways to increase the area of unrepaired IRIF in the IR+HT group. (A) Representative time-lapse images show the growth in individual IRIF area *in situ* (white arrows). Bar = 5 μm. (B) Representative images of the merging of adjacent IRIF in the *x–y* plane (upper panel) and *x–z* plane (lower panel). White arrows show the clustering process of the proximal IRIF. Bar = 5 μm.

(41°C) efficiently induces degradation of BRCA2 and inhibits HR [8]. The inhibition of HR might stimulate the NHEJ or backup pathways of NHEJ [16–18] that was responsible for the error-prone repair [19]. Whether IR+HT causes more misrepaired DSBs in HT1080 cells is still unclear; therefore, further studies need to be performed by evaluating the induction of chromosome rearrangements.

Interestingly, through *in situ* tracking of individual IRIF from the IR+HT group, we found that HT resulted in more unrepaired IRIF over the period of observation compared with treatment with IR alone. Additionally, the unrepaired IRIF had a larger area and a higher intensity as well as a slower repair rate (Fig. 3). Previous studies have shown that larger IRIF may represent the machinery for slower repair of complex DSBs [20]. Moreover, larger IRIF are more persistent and are closely correlated with cell lethality [21]. Moreover, low-intensity foci are believed to represent simple DSBs, which are repaired quickly [22]. If the IRIF were always persistent in the nucleus, they can be viewed as 'residual IRIF'. Several previous studies have reported a possible correlation between residual IRIF and cellular radiosensitivity [21, 23]. Furthermore, based on *in situ* tracking of individual IRIF, we found that the apparent change in area of unrepaired IRIF was mainly due to the area of individual IRIF increasing, rather than the clustering of proximal IRIF (Fig. 4). This could result in relocalizing of repair proteins to persisting lesions [24], or the expansion of chromatin in the vicinity of DSBs [25].

In summary, we found that HT could delay and decrease the formation of 53BP1 IRIF. Additionally, almost every heated cell contained a type of IRIF displaying larger area, higher intensity and slower repair rate compared with the unheated cells. Moreover, the majority of these IRIF had an apparent increase in area. Our results suggested that HT could perturb the primary event of the DDR induced by IR, and this may be responsible for the heated cells' inability to repair DSBs.

CONFLICT OF INTEREST

No potential conflicts of interest were disclosed.

REFERENCES

1. Wust P, Hildebrandt B, Sreenivasa G et al. Hyperthermia in combined treatment of cancer. *Lancet Oncol* 2002;3:487.
2. Horsman MR, Overgaard J Hyperthermia: a potent enhancer of radiotherapy. *Clin Oncol* 2007;19:418–26.
3. Dikomey E, Becker W, Wielckens K Reduction of DNA-polymerase β activity of CHO cells by single and combined heat treatments. *Int J Radiat Biol Relat Stud Phys Chem Med* 1987;52:775–85.
4. Chapman JR, Taylor MR, Boulton SJ Playing the end game: DNA double-strand break repair pathway choice. *Mol Cell* 2012;47:497–510.
5. Burgman P, Ouyang H, Peterson S et al. Heat inactivation of Ku autoantigen: possible role in hyperthermic radiosensitization. *Cancer Res* 1997;57:2847–50.
6. Seno JD, Dynlacht JR. Intracellular redistribution and modification of proteins of the Mre11/Rad50/Nbs1 DNA repair complex following irradiation and heat-shock. *J Cell Physiol* 2004;199:157–70.
7. San FJ, Sung P, Klein H. Mechanism of eukaryotic homologous recombination. *Annu Rev Biochem* 2008;77:229–57.
8. Krawczyk PM, Eppink B, Essers J et al. Mild hyperthermia inhibits homologous recombination, induces BRCA2 degradation, and sensitizes cancer cells to poly (ADP-ribose) polymerase-1 inhibition. *Proc Natl Acad Sci U S A* 2011;108:9851–6.
9. Laszlo A, Fleischer I Heat-induced perturbations of DNA damage signaling pathways are modulated by molecular chaperones. *Cancer Res* 2009;69:2042.
10. Asaithamby A, Chen DJ Cellular responses to DNA double-strand breaks after low-dose gamma-irradiation. *Nucleic Acids Res* 2009;37:3912.
11. Y Liang, Q Fu, W Wang et al. An integrated on-line irradiation and *in situ* live cell imaging system. *Nucl Instrum Methods B* 2015;358:26–31.
12. Hunt CR, Pandita RK, Laszlo A et al. Hyperthermia activates a subset of ataxia-telangiectasia mutated effectors independent of DNA strand breaks and heat shock protein 70 status. *Cancer Res* 2007;67:3010–17.
13. Schultz LB, Chehab NH, Malikzay A et al. P53 binding protein 1 (53bp1) is an early participant in the cellular response to DNA double-strand breaks. *J Cell Biol* 2000;151:1381–90.
14. Kampinga HH, Hiemstra YS, Konings AW et al. Correlation between slowly repairable double-strand breaks and thermal radiosensitization in the human HeLa S3 cell line. *Int J Radiat Biol* 1997;72:293–301.
15. Kampinga HH, Dikomey E Hyperthermic radiosensitization: mode of action and clinical relevance. *Int J Radiat Biol* 2001;77:399–408.
16. Kim J-S, Krasieva TB, Kurumizaka H et al. Independent and sequential recruitment of NHEJ and HR factors to DNA damage sites in mammalian cells. *J Cell Biol* 2005;170:341–7.
17. Rodrigue A, Lafrance M, Gauthier MC et al. Interplay between human DNA repair proteins at a unique double-strand break *in vivo*. *EMBO J* 2006;25:222–31.
18. Wu W, Wang M, Wu W et al. Repair of radiation induced DNA double strand breaks by backup NHEJ is enhanced in G2. *DNA Repair* 2008;7:329–38.
19. Bergs JW, Krawczyk PM, Borovski T et al. Inhibition of homologous recombination by hyperthermia shunts early double strand break repair to non-homologous end-joining. *DNA Repair* 2013;12:38–45.

20. Belyaev IY Radiation-induced DNA repair foci: spatio-temporal aspects of formation, application for assessment of radiosensitivity and biological dosimetry. *Mutat Res* 2010;704:132–41.

21. Banáth JP, Klokov D, MacPhail SH et al. Residual γH2AX foci as an indication of lethal DNA lesions. *BMC Cancer* 2010;10:4.

22. Antonelli F, Campa A, Esposito G et al. Induction and repair of DNA DSB as revealed by H2AX phosphorylation foci in human fibroblasts exposed to low- and high-LET radiation: relationship with early and delayed reproductive cell death. *Radiat Res* 2015;183:417–31.

23. Rothkamm K, Löbrich M. Evidence for a lack of DNA double-strand break repair in human cells exposed to very low x-ray doses. *Proc Natl Acad Sci U S A* 2003;100:5057–62.

24. Nelms BE, Maser RS, MacKay JF et al. In situ visualization of DNA double-strand break repair in human fibroblasts. *Science* 1998;280:590.

25. Kruhlak MJ, Celeste A, Dellaire G et al. Changes in chromatin structure and mobility in living cells at sites of DNA double-strand breaks. *J Cell Biol* 2006;172:823.